Exhibit 1- References

[1] World Meteorological Organization, 2003: *Manual on the Global Observing System*. WMO-No. 544, Geneva.

[2] World Meteorological Organization, 2008: *Guide to Meteorological Instruments and Methods of Observation, Part I Chapter 5: Measurement of Surface Wind.* WMO-No. 8, Geneva.

[3] World Meteorological Organization, 2008: *Guide to Meteorological Instruments and Methods of Observation, Part II Chapter 1: Measurements at Automatic Weather Stations.* WMO-No. 8. Geneva.

[4] Peterka, J.A. and M. Poreh, Siting Guidelines for Low Level Windshear Alert System (LLWAS) Remote Facilities, for the Federal Aviation Administration (FAA), FAA Order 6560.21A, 1989.

[5] National Wildfire Coordinating Group, 2008: *NWCG Fire Weather Station Standards.*

[6] ESDU (1993a) Strong winds in the atmospheric boundary layer, Part 1: mean hourly wind speeds, ESDU Report 82026, ESDU International.

[7] ESDU (1993b) Strong winds in the atmospheric boundary layer, Part 2: discrete gust speeds, ESDU Report 83045, ESDU International.

[8] Cermak, J.E. (1971), "Laboratory Simulation of the Atmospheric Boundary Layer," *AIAA Jl.*, Vol. 9, September.

[9] Cermak, J.E. (1975), "Applications of Fluid Mechanics to Wind Engineering," A Freeman Scholar Lecture, *ASME Journal of Fluids Engineering*, Vol. 97, No. 1, March.

[10] Cermak, J.E. (1976), "Aerodynamics of Buildings," *Annual Review of Fluid Mechanics*, Vol. 8, pp. 75 – 106.

[11] Meroney, R. N. (1980), A Wind-Tunnel Simulation of the Flow Over Hills and Complex Terrain, Journal of Industrial Aerodynamics, Vol. 5, pp 297-321.

[12] Barlow, J.B., W.H. Rae, A. Pope (1999), Low-Speed Wind Tunnel Testing, Wiley-Interscience, pp 1-728

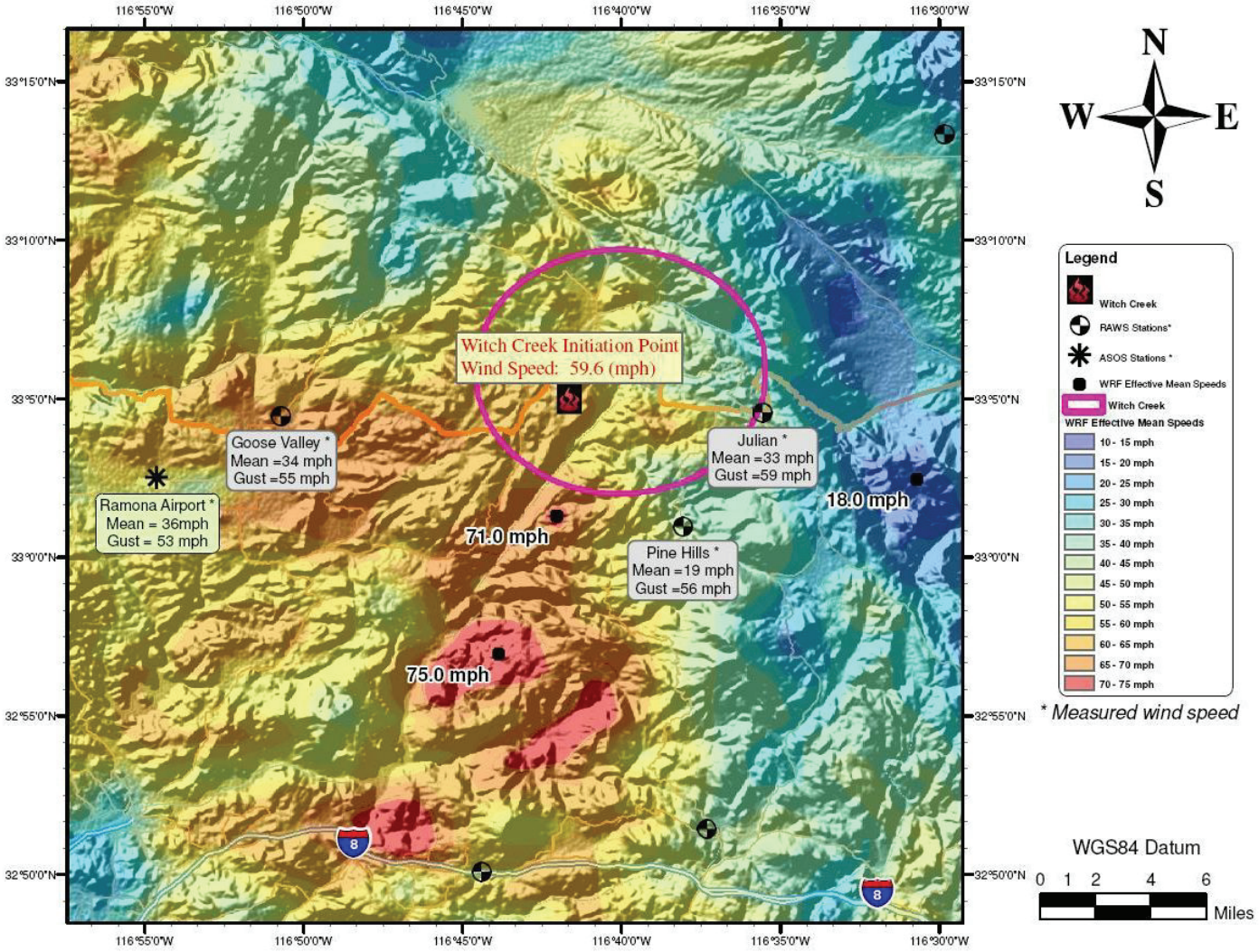

Exhibit 2. Wind speeds determined by WRF analysis at 10 m above the ground surface.

Exhibit 3a. Witch Creek wind tunnel model test turntable with upwind terrain.

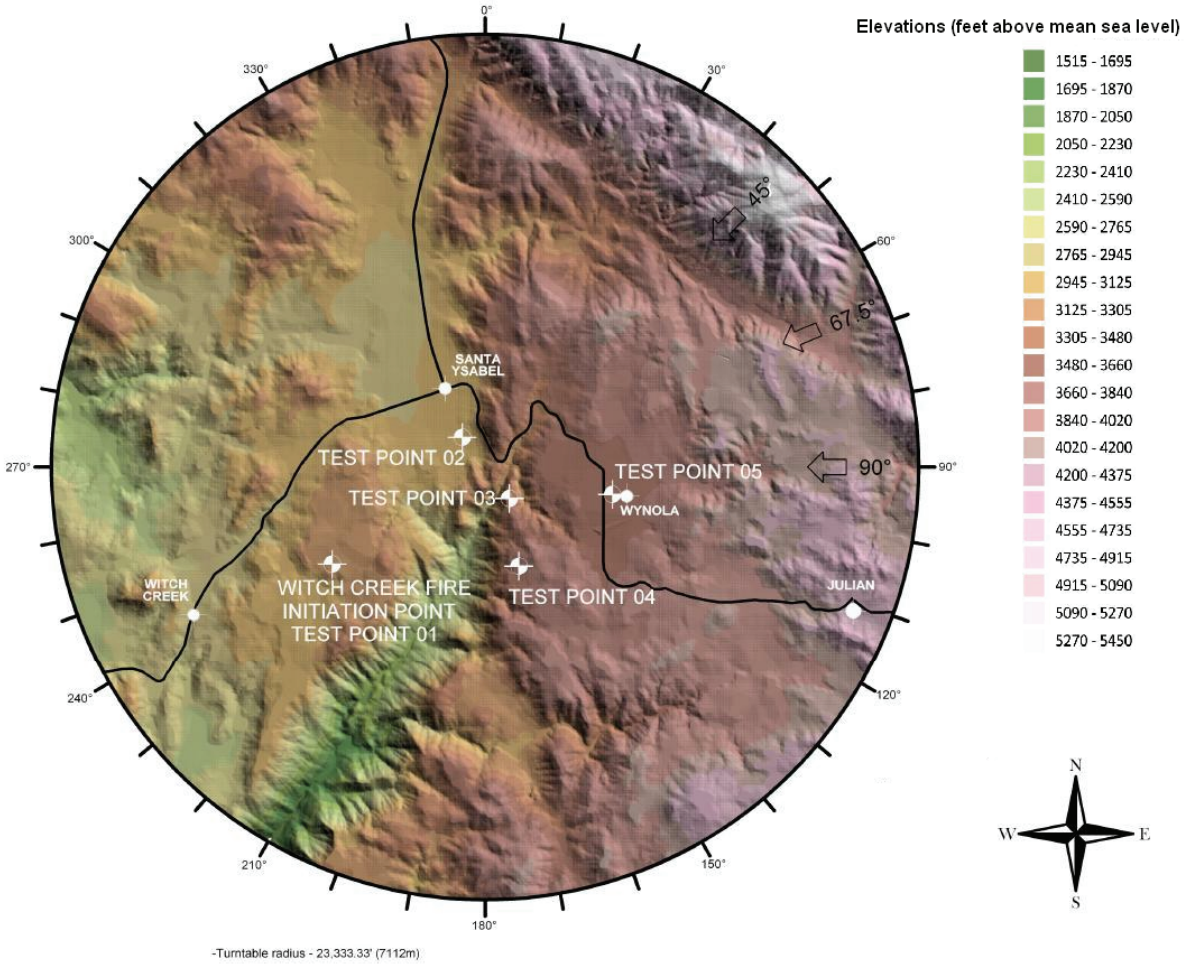

Exhibit 3b. Witch Creek wind tunnel model test turntable with upwind terrain.

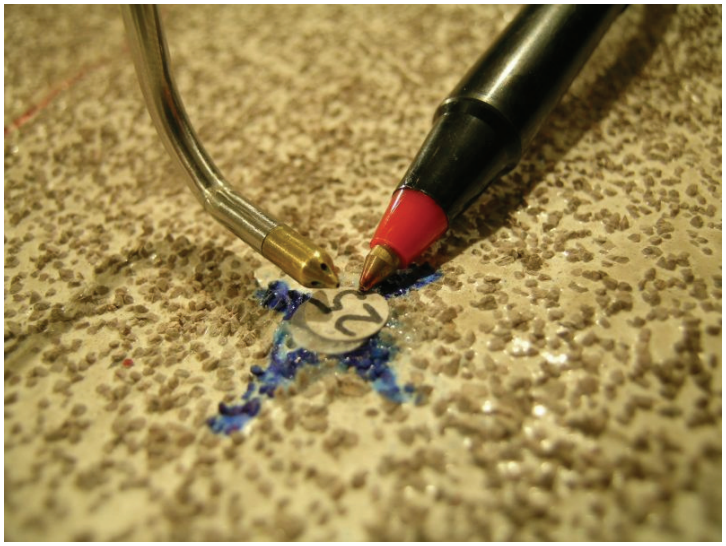

Exhibit 3c. Measurement probe to sample 3 components of velocity.

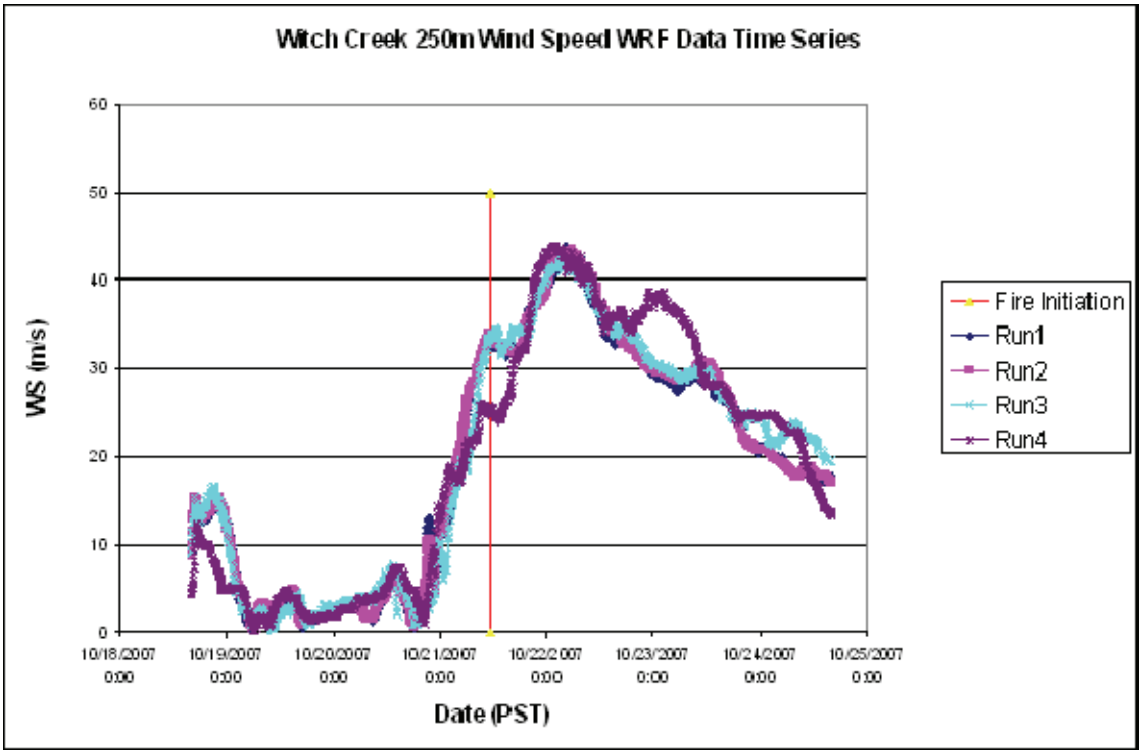

Exhibit 4. WRF 250m wind speed time histories for all four runs.

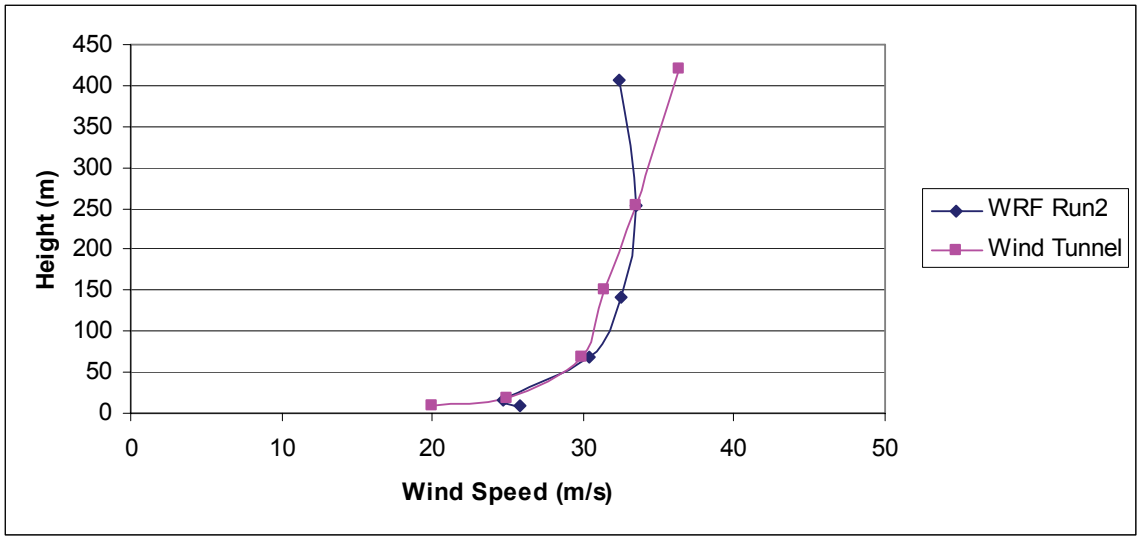

Exhibit 5. WRF wind speed profiles for the fire initiation time.

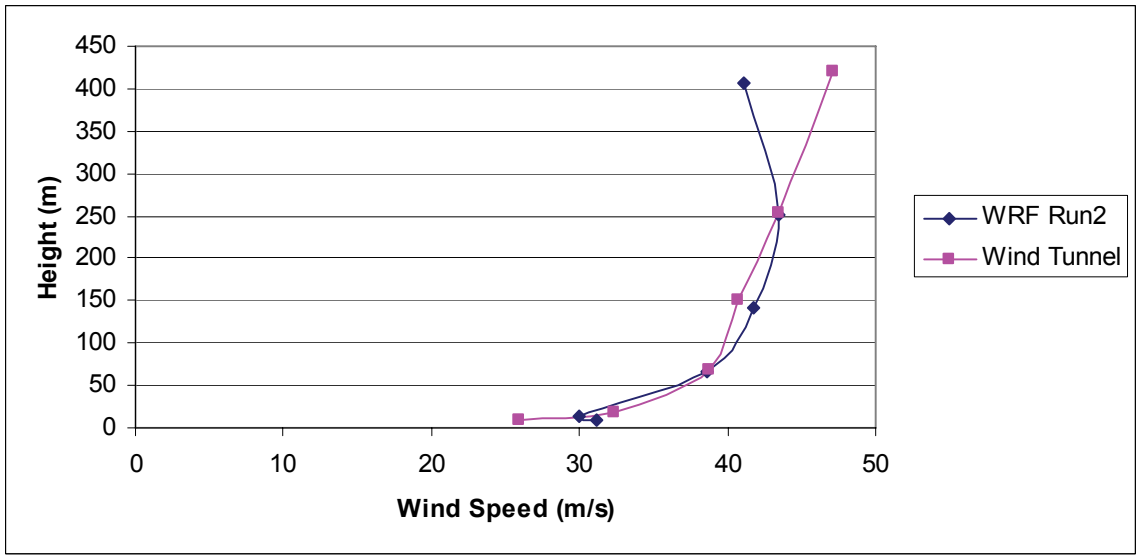

Exhibit 6. WRF wind speed profiles at the time of the peak 250m wind speed.

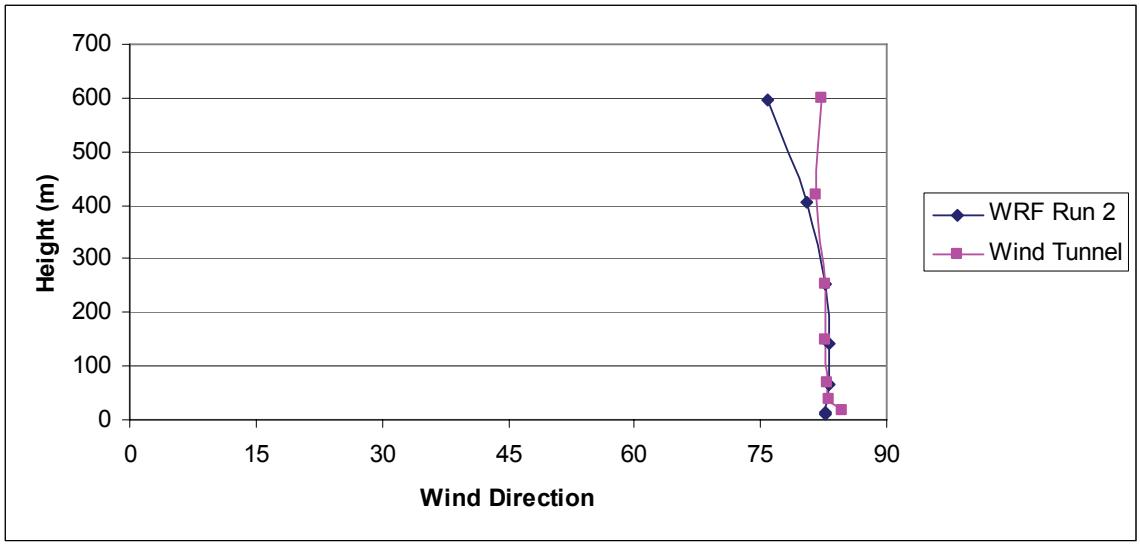

Exhibit 7. WRF wind direction profiles for the fire initiation time.

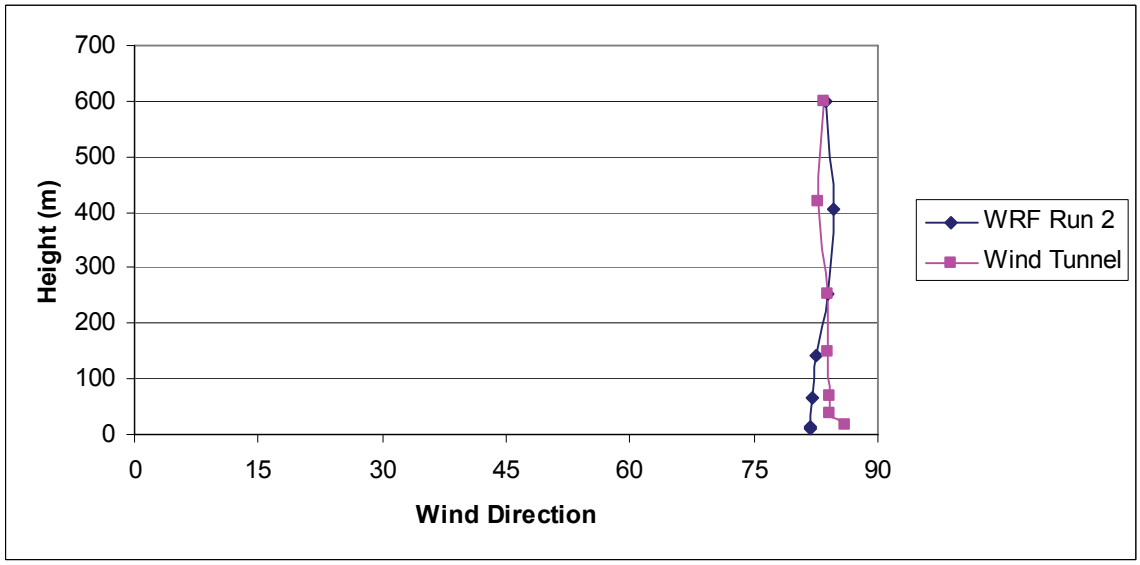

Exhibit 8. WRF wind direction profiles at the time of the peak 250m wind speed.

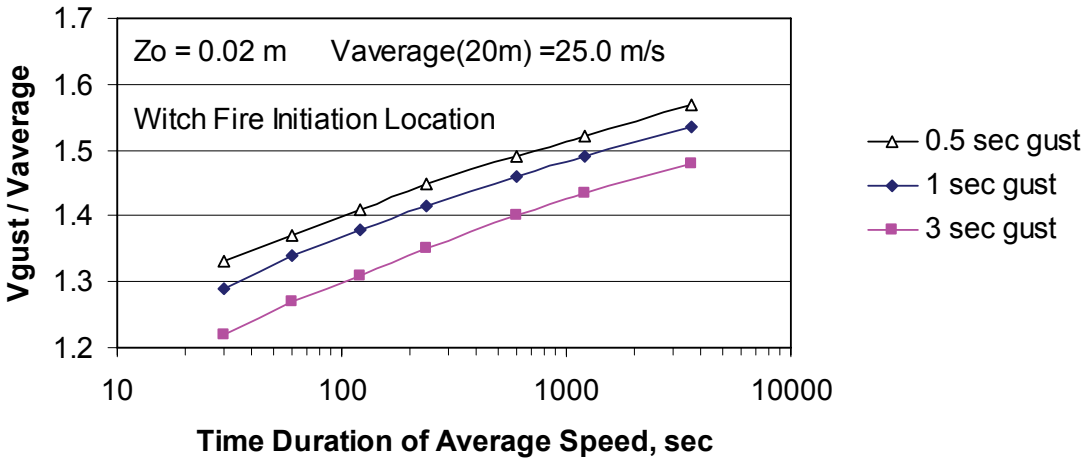

Exhibit 9. Gust factor as a function of averaging times for mean and gust.

Exhibit 10a. Julian anemometer location; note sheltering trees and structures surrounding site on all sides.

Exhibit 10b. Julian anemometer location and location of photographs JULC1-1, JULC1-2, JULC1-3, JULC1-4, and JULC1-5 with wind direction range during the Santa Ana event; note sheltering trees and structures upwind of anemometer.

Exhibit 11a. Photograph JULC1-1 looking SSW (see Exhibit 10b).

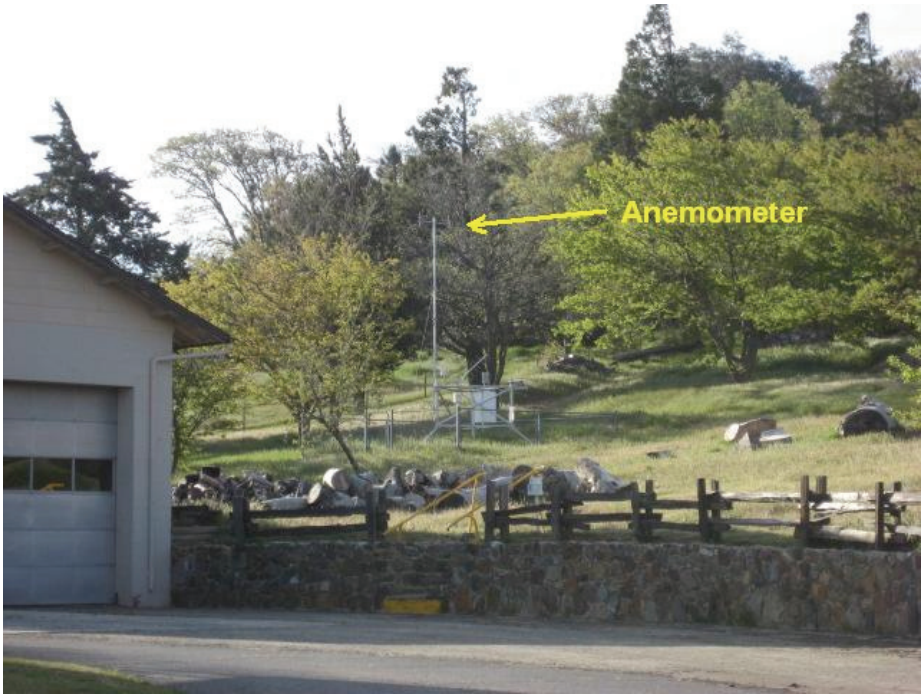

Exhibit 11b. Photograph JULC1-2 looking SE (see Exhibit 10b).

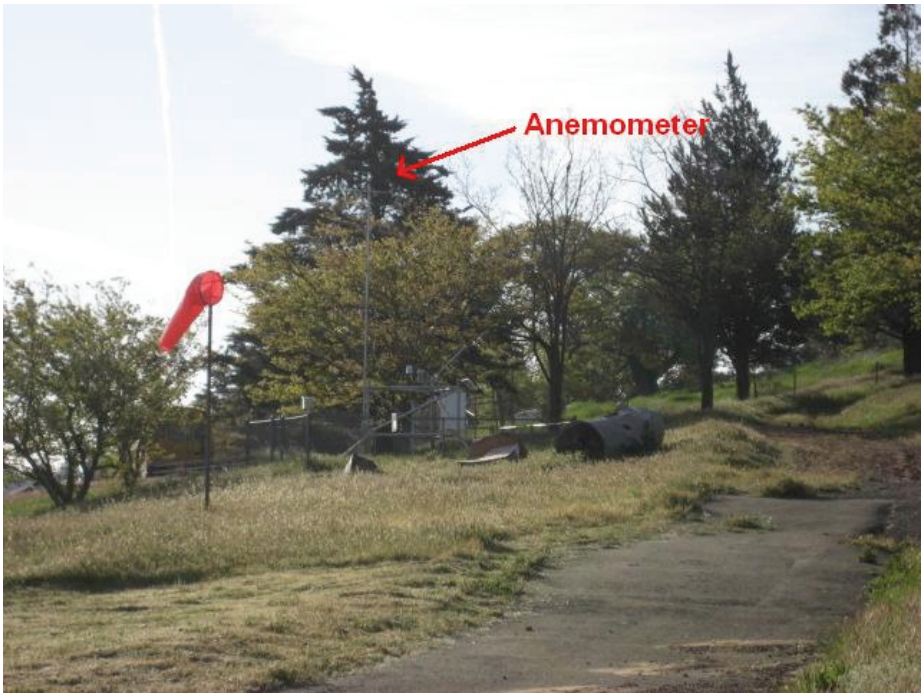

Exhibit 11c. Photograph JULC1-3 looking ESE (see Exhibit 10b).


Exhibit 11d. Photograph JULC1-4 looking NE (see Exhibit 10b).

Exhibit 11e. Photograph JULC1-5 looking E (see Exhibit 10b).